Binding-activated localization microscopy of DNA structures

Schoen, Ingmar ; Ries, Jonas ; Klotzsch, Enrico ; Ewers, Helge ; Vogel, Viola

Abstract: Many nucleic acid stains show a strong fluorescence enhancement upon binding to double-stranded DNA. Here we exploit this property to perform superresolution microscopy based on the localization of individual binding events. The dynamic labeling scheme and the optimization of fluorophore brightness yielded a resolution of 14 nm (fwhm) and a spatial sampling of 1/nm. We illustrate our approach with two different DNA-binding dyes and apply it to visualize the organization of the bacterial chromosome in fixed Escherichia coli cells. In general, the principle of binding-activated localization microscopy (BALM) can be extended to other dyes and targets such as protein structures.

DOI: https://doi.org/10.1021/nl2025954

Binding-Activated Localization Microscopy of DNA Structures

Ingmar Schoen[1,3], Jonas Ries[2,3], Enrico Klotzsch[1], Helge Ewers[2,4], Viola Vogel[1,4]

[1] Laboratory for Biologically Oriented Materials, ETH Zurich, Zurich, Switzerland;

[2] Institute of Biochemistry, ETH Zurich, Zurich, Switzerland;

[3] these authors contributed equally to this work;

[4] these authors contributed equally to this work;

* to whom correspondence should be addressed: ingmar.schoen@mat.ethz.ch

ABSTRACT Many nucleic acid stains show a strong fluorescence enhancement upon binding to double-stranded DNA. Here we exploit this property to perform superresolution microscopy based on the localization of individual binding events. The dynamic labeling scheme and the optimization of fluorophore brightness yielded a resolution of ~14 nm (FWHM) and a spatial sampling of 1/nm. We illustrate our approach with two different DNA-binding dyes and apply it to visualize the organization of the bacterial chromosome in fixed *E.coli* cells. In general, the principle of binding-activated localization microscopy (BALM) can be extended to other dyes and targets such as protein structures.

KEYWORDS intercalating dyes, PALM, STORM, nucleoid, YOYO-1, PicoGreen

MANUSCRIPT TEXT

Localization microscopy of extended biological structures relies on the separation of the fluorescence emission from individual molecules inside a diffraction-limited spot by sequentially bringing them into bright states. The resolution in common approaches is limited by the number of photons per dye molecule when using photo-activatable proteins (PALM[1]) and by the labeling density due to an insufficient ratio between dark and bright fluorophores when using organic dyes (STORM[2], blinking[3, 4]). Here we improve upon both localization accuracy and density by utilizing fluorophores that are 'switched on' upon binding to a target structure and directly exploit this property to localize them under dynamic binding conditions (Figure 1). Repeated cycles of binding, localization, and bleaching allow the optical reconstruction of the biological structure under investigation. This strategy termed here binding-activated localization microscopy (BALM) can be generalized to visualize biological or synthetic structures with nanoscale resolution using a variety of available dyes.

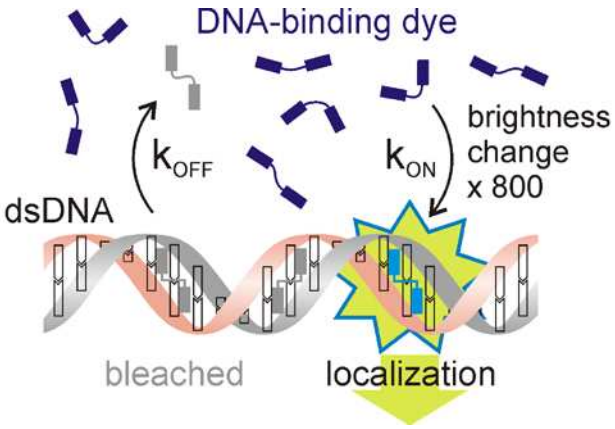

Figure 1. Binding-Activated Localization Microscopy (BALM). Free dyes turn bright upon binding to a target structure and can be localized with sub-diffraction resolution before they eventually bleach or detach. Molecules detach from the DNA with an off rate k_{off}, whereas the binding kinetics are determined by the on rate k_{on} and the dye concentration in solution. Images are taken using a wide-field microscope and a sensitive EM-CCD camera.

In this work, we utilize DNA-binding dyes that show a fluorescence enhancement by three orders of magnitude when bound to double-stranded DNA. The dimeric dye YOYO-1[3] intercalates in-between successive base pairs along the DNA double helix[4]. In solution, its fluorescence is strongly quenched by

internal rotational motion of its chromophores[4]. Upon binding, the chromophores become immobilized and the quantum yield increases by about 800 times. YOYO-1 has already been used for superresolution imaging of DNA molecules: Flors and coworkers induced dye blinking by adding cysteamine to the imaging buffer for blinking microscopy[5-7], whereas Hell and coworkers used YOYO-1 for stimulated emission depletion (STED) microscopy[8]. Both studies used pre-labeled DNA and reached a resolution of 35-50 nm. Tinnefeld and coworkers utilized the transient binding of hybridizing ssDNA strands for a sequence-specific mapping of DNA origamis[9]. However, none of above approaches yielded high localization accuracy and high labeling density at the same time. Here we overcome this shortcoming by taking advantage of the intrinsic fluorescence enhancement of YOYO-1 and a dynamic labeling scheme where the dye brightness can be systematically optimized and the labeling density can be tuned nearly at will.

DNA from lambda phage was spincoated onto polylysine-coated coverslips[7]. YOYO-1 was added to the imaging buffer and images were taken at a rate of 20 s^{-1}. Dark molecules in solution became bright upon binding and were localized only then. Accumulated localizations allowed for the optical reconstruction of stretched dsDNA molecules (Fig. 2 a) with a full width at half maximum (FWHM) of 37 nm (Fig. 3 c) and a mean density of one localization per 15 nm (Fig. 3 d). The frequency of binding events was controlled by the dye concentration in solution.

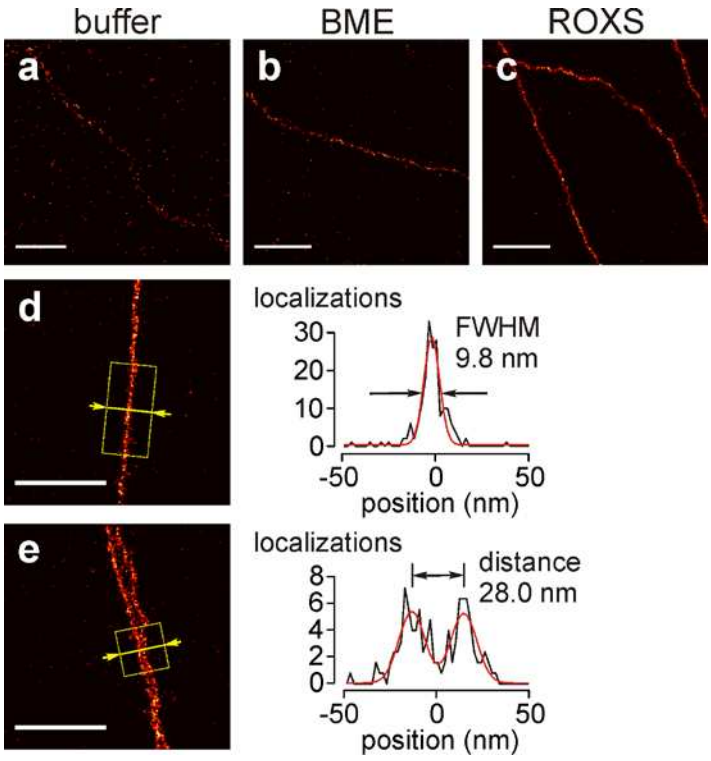

Figure 2. Superresolution imaging of DNA molecules with the DNA-intercalating dye YOYO-1. Reconstructed image of spin-coated λ-DNA recorded under total internal reflection (TIR) illumination in buffer (a), buffer with 4% β-mercapto ethanol (BME) (b), or buffer containing 10 mM ascorbic acid and 1 mM methyl viologen (ROXS) (c-e). Scalebars 200 nm, YOYO-1 concentrations: 1 nM (a,b) or 0.1 nM (c-e). (d,e) Line profiles for determining the full width half maximum (FWHM) and resolution limit. The analyzed segment lengths were 200 nm (f) and 100 nm (g), respectively (dashed boxes).

Optimizing the buffer-conditions with respect to brightness and binding kinetics can be used to greatly increase the resolution. Several strategies have been reported to enhance the brightness and lifetime of fluorophores that rely on quenching of the triplet state or other dark states by chemical reactions [10-14]. In our case, both the addition of β-mercapto ethanol (BME) (Fig. 2 b) or a reducing-oxidizing system (ROXS)[11] (Fig. 2 c) containing ascorbic acid and methyl viologen led to a 2-3 fold increase in brightness (Supplementary Fig. 1) resulting in an improved FWHM of ~14 nm (Fig. 2 d, Fig. 3 c). This made it possible to resolve two DNA molecules at a separation below 30 nm (Fig. 2 e). The fixed orientation of the fluorophore affected the achievable precision only to a minor extent (see Supplementary Information). As a positive side effect, both BME and ascorbic acid are known to protect DNA against photodamage that accompanies dye bleaching [15-17].

Furthermore, we found that the different buffer conditions affected the interaction of YOYO-1 with dsDNA. BME speeded up the binding kinetics (Fig. 3 a) but had no observable effect on the detachment of YOYO-1 from the DNA (Fig. 3 b). This behavior can be explained by an effective reduction of the solubility of YOYO-1 in BME-containing buffer. In contrast, ROXS enhanced both on- and off-rates dramatically (Fig. 3 a,b), indicating a competitive interaction with the base pairs[18]. As a result the DNA structure is continuously targeted by dyes from solution and freed from bleached dyes. Under these conditions, a spatial sampling of the DNA contour with nearly one localization per nm was achieved (Fig. 3 d) which constitutes an improvement by more than one order of magnitude when compared to conventional labeling strategies[1, 2, 11, 19, 20].

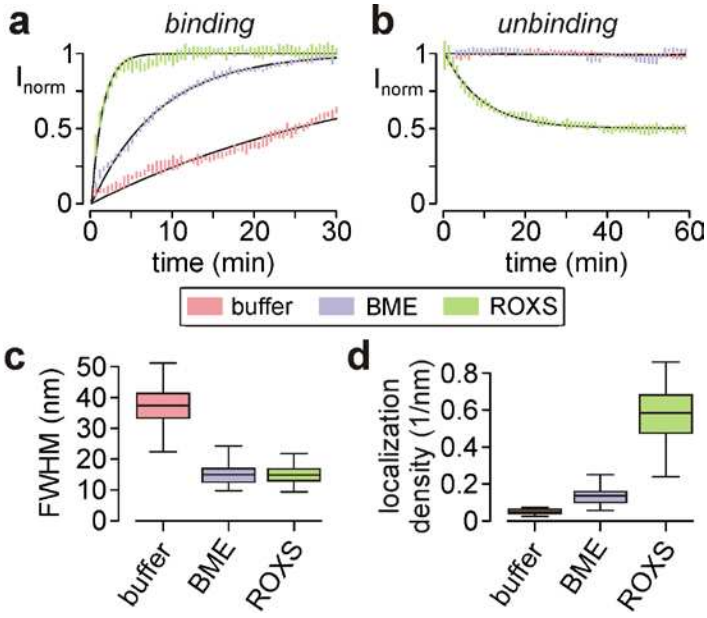

Figure 3. Dynamic labeling of DNA with YOYO-1 and imaging resolution under different buffer conditions. (a,b) Time-lapse measurements of (a) binding kinetics (at 1 nM) and (b) unbinding kinetics of YOYO-1 under the indicated buffer conditions. Error bars: standard error of the mean from five different DNA molecules. Lines: single exponential fits to the data. Binding time constants τ = 36 min (buffer), τ = 8.4 min (BME), τ = 1.4 min (ROXS), unbinding τ = 9 min (ROXS). (c,d) Statistical analysis of imaging resolution with YOYO-1. Box-whisker plots for the FWHM (a) and localization density along DNA strands (b) with n = 21 (buffer), n = 39 (BME), and n = 79 (ROXS). Boxes represent mean, lower and upper quartile of the distributions, whiskers depict smallest and largest values in each data set.

To demonstrate the versatility of the BALM principle we used the fluorophore PicoGreen[21, 22] that has a completely different binding mechanism with the major groove of the DNA double helix as its binding site. PicoGreen shows similar fluorescence enhancement of about 1000 fold but has higher selectivity of dsDNA over RNA, making it especially interesting for imaging in cells. Under normal buffer conditions we found that PicoGreen molecules were dim and bleached fast (data not shown). Addition of ROXS dramatically enhanced the brightness and lifetime, enabling the imaging of DNA molecules with a FWHM of 26.7±4.7 nm (Fig. 4) and a localization density of 0.41±0.08 nm^{-1} (n = 29). Compared with YOYO-1, PicoGreen was not as bright but reached a similar labeling density along the DNA. Hence we conclude that both the BALM principle as well as the buffer optimization strategy can be extended to other dyes.

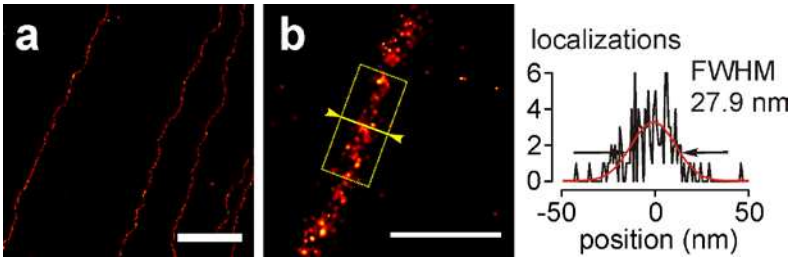

Figure 4. Superresolution imaging of DNA molecules with the dye PicoGreen that binds to the major groove. (a) Reconstructed image of spin-coated λ-DNA recorded in ROXS buffer with 150 pM PicoGreen. Scale bar 1 µm. (b) Line profile for determining the FWHM. The analyzed segment length was 200 nm (dashed box). Scale bar: 200 nm.

To demonstrate the capability of resolving biological DNA structures in more complex environments, we investigated the chromosomal organization in bacteria. Up to now, bacterial chromosome structure has been studied mainly by conventional light microscopy or by AFM on lysed cells[23, 24]. These approaches were limited by either the resolution or by possible preparation artifacts. Hence, the organization of the nucleoid inside bacterial cells is still elusive and a matter of an ongoing debate[25, 26].

We used BALM with PicoGreen to image chromosomal organization in fixed *Escheria coli* cells (Fig. 5). Movies were taken at a frame rate of 66 s^{-1} using 10-50 pM PicoGreen in ROXS buffer. A significant fraction of DNA-bound PicoGreen molecules showed diffusive motion, suggesting that even in fixed bacteria, part of the DNA is still dynamic which resulted in a homogenous background. Despite

these shortcomings, the reconstructed images clearly show the dramatic enhancement in resolution when compared with diffraction-limited microscopy (Fig. 5 a,b). The chromosome in these cells was elongated over the whole cell length and the overall contour of the nucleoid inside the right cell was slightly curled. Daughter chromosomes in two nascent cells showed a clustering near the site of cell division (Fig. 5 c) whereas at a later stage they were fully separated (Fig. 5 e). Chromosomes showed a striking heterogeneity on sub-wavelength length scales. Details include void regions on the order of ~100 nm (cyan arrowheads) or filamentous structures (white arrowheads, Fig. 5 d,f). Overall, BALM with PicoGreen enables the investigation of the bacterial nucleoid within fixed cells with unprecedented resolution.

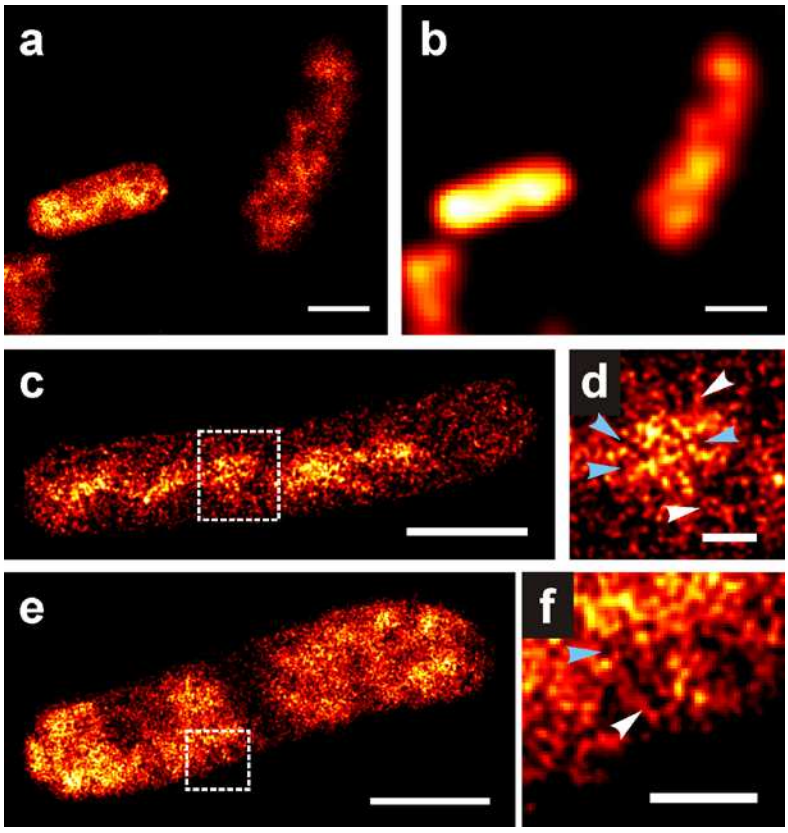

Figure 5. BALM imaging of nucleoid organization in fixed bacteria with PicoGreen. (a) BALM image. (b) Diffraction-limited rendering of (a). (c,e) Dividing cells. (d,f) Magnified views of the regions in dashed boxes from figures (c,e), respectively. The arrowheads point out small void regions (cyan) or filamentous structures (white). Scale bars: 1 µm (a-c,e) or 200 nm (d,f).

Future applications of BALM with DNA-binding dyes will help to elucidate the structural organization of chromosomes in bacteria depending on growth conditions, proliferation state or special

RNAase treatments[24]. The spectral characteristics of YOYO-1 and PicoGreen with excitation in the blue and emission in the green also allow the combination with longer-wavelength probes. For example, protein-DNA colocalization could be studied with a precision of few base pairs using BALM with YOYO-1 and PALM with genetically encoded fluorescent protein tags.

Another compelling task would be to resolve the fixed orientation of intercalating dyes along the DNA double helix by using an objective with a very high numerical aperture (NA 1.6) and implementing the description of a fixed dipole as the point spread function for fitting[27]. Together with the nm-dense labeling of BALM, the measurement of the helical pitch of dsDNA molecules should be in reach.

In general, various fluorophores show fluorescence enhancement or spectral shifts upon integration into a biological target structure. Examples are the membrane-binding dye Nile red[28] or the complementation assay based on the split-GFP system[29] that hold the potential to extend BALM to membranes or specific protein structures. Moreover, molecular beacons[30] could be used for BALM to map dsDNA structures in a sequence-specific manner. We expect that the discovery of further BALM probes will enable localization microscopy with nm resolution and ultra dense labeling in various biological systems.

Acknowledgments: We thank Philippe Emge for help with bacterial preparations, Henrik Flyvbjerg, Jan Vogelsang, and Britta Person-Skegro for discussions and Wesley Legant for comments on the manuscript. This work was supported by a Marie Curie Intra-European Fellowship (JR) and an ERC Advanced Grant (VV) within the 7th European Framework Program, the NCCR Neural Plasticity and Repair (HE) and by ETH Zurich.

Supporting Information Available. Detailed materials and methods, additional figures and a detailed discussion of the localization accuracy accompany this article. This material is available free of charge via the Internet at http://pubs.acs.org.

REFERENCES

1. Betzig, E.; Patterson, G. H.; Sougrat, R.; Lindwasser, O. W.; Olenych, S.; Bonifacino, J. S.; Davidson, M. W.; Lippincott-Schwartz, J.; Hess, H. F. *Science* **2006,** 313, (5793), 1642-1645.

2. Bates, M.; Dempsey, G. T.; Zhuang, X. W. *Science* **2007,** 317, (5845), 1749-1753.

3. Glazer, A. N.; Rye, H. S. *Nature* **1992,** 359, (6398), 859-861.

4. Ihmels, H.; Otto, D. *Supermol. Dye Chem.* **2005,** 258, 161-204.

5. Flors, C. *Biopolymers* **2010,** 95, (5), 290-297.

6. Flors, C. *Photochem. Photobiol. Sci.* **2010,** 9, (5), 643-648.

7. Flors, C.; Ravarani, C. N. J.; Dryden, D. T. F. *ChemPhysChem* **2009,** 10, (13), 2201-2204.

8. Persson, F.; Bingen, P.; Staudt, T.; Engelhardt, J.; Tegenfeldt, J. O.; Hell, S. W. *Angew. Chem. Int. Edit.* **2011,** 50, (24), 5581-5583.

9. Jungmann, R.; Steinhauer, C.; Scheible, M.; Kuzyk, A.; Tinnefeld, P.; Simmel, F. C. *Nano Lett.* **2010,** 10, (11), 4756-4761.

10. Campos, L. A.; Liu, J. W.; Wang, X.; Ramanathan, R.; English, D. S.; Munoz, V. *Nat. Methods* **2011,** 8, (2), 143-U63.

11. Vogelsang, J.; Steinhauer, C.; Forthmann, C.; Stein, I. H.; Person-Skegro, B.; Cordes, T.; Tinnefeld, P. *ChemPhysChem* **2010,** 11, (12), 2475-2490.

12. Gurrieri, S.; Wells, K. S.; Johnson, I. D.; Bustamante, C. *Anal. Biochem.* **1997,** 249, (1), 44-53.

13. Vogelsang, J.; Kasper, R.; Steinhauer, C.; Person, B.; Heilemann, M.; Sauer, M.; Tinnefeld, P. *Angew. Chem. Int. Edit.* **2008,** 47, (29), 5465-5469.

14. Widengren, J.; Chmyrov, A.; Eggeling, C.; Lofdahl, P. A.; Seidel, C. A. M. *J. Phys. Chem. A* **2007,** 111, (3), 429-440.

15. Cosa, G.; Focsaneanu, K. S.; McLean, J. R. N.; McNamee, J. P.; Scaiano, J. C. *Photochem. Photobiol.* **2001,** 73, (6), 585-599.

16. Kanony, C.; Akerman, B.; Tuite, E. *J. Am. Chem. Soc.* **2001,** 123, (33), 7985-7995.

17. Yoshikawa, Y.; Hizume, K.; Oda, Y.; Takeyasu, K.; Araki, S.; Yoshikawa, K. *Biophys. J.* **2006,** 90, (3), 993-999.

18. Neault, J. F.; Naoui, M.; Tajmirriahi, H. A. *J. Biomol. Struct. Dyn.* **1995,** 13, (2), 387-397.

19. van de Linde, S.; Wolter, S.; Heilemann, M.; Sauer, M. *J. Biotechnol.* **2010,** 149, (4), 260-266.

20. Greenfield, D.; McEvoy, A. L.; Shroff, H.; Crooks, G. E.; Wingreen, N. S.; Betzig, E.; Liphardt, J. *PLoS. Biol.* **2009,** 7, (6).

21. Dragan, A. I.; Casas-Finet, J. R.; Bishop, E. S.; Strouse, R. J.; Schenerman, M. A.; Geddes, C. D. *Biophys. J.* **2010,** 99, (9), 3010-3019.

22. Schneeberger, C.; Speiser, P.; Kury, F.; Zeillinger, R. *PCR-Methods Appl.* **1995,** 4, (4), 234-238.

23. Dame, R. T. *Mol. Microbiol.* **2005,** 56, (4), 858-870.

24. Ohniwa, R. L.; Morikawa, K.; Takeshita, S. L.; Kim, J.; Ohta, T.; Wada, C.; Takeyasu, K. *Genes Cells* **2007,** 12, (10), 1141-1152.

25. Bendich, A. J. *Biochimie* **2001,** 83, (2), 177-186.

26. Thanbichler, M.; Wang, S. C.; Shapiro, L. *J. Cell. Biochem.* **2005,** 96, (3), 506-521.

27. Mortensen, K. I.; Churchman, L. S.; Spudich, J. A.; Flyvbjerg, H. *Nat. Methods* **2010,** 7, (5), 377-381.

28. Sharonov, A.; Hochstrasser, R. M. *Proc. Natl. Acad. Sci. U.S.A.* **2006,** 103, (50), 18911-18916.

29. Pinaud, F.; Dahan, M. *Proc. Natl. Acad. Sci. U.S.A.* **2011,** 108, (24), E201-E210.

30. Tyagi, S.; Bratu, D. P.; Kramer, F. R. *Nat. Biotechnol.* **1998,** 16, (1), 49-53.

SYNOPSIS TOC GRAPHIC